

## Grain size distributions in airborne dust, river-suspended loads, and marine sediments from southeastern Turkey (NE Mediterranean Sea)

Vedat EDİGER\*\*\*

Earth and Marine Sciences Institute, TÜBİTAK MAM, Gebze, Kocaeli, Turkey

Received: 25.02.2020 • Accepted/Published Online: 03.07.2020 • Final Version: 04.09.2020

**Abstract:** Between February 2001 and January 2002, near the coast of Erdemli, southeastern Turkey, 7 airborne dust samples, 7 coastal river-suspended sediment samples, and 3 marine sediment cores were collected. The main objective of this study was to understand the interrelationships among the multisources, multitransportation paths, and changing depositional conditions around the continental shelf of the Lamas River delta. In addition to a detailed study of satellite photos to track atmospheric dust in the region, grain size analyses were conducted on airborne dust, riverine suspensions, and marine sediment (cores), and the results were interpreted using statistical data, such as mean, mode, sorting, skewness, and kurtosis. The bimodal grain size distributions of the airborne dust indicated higher rates of clayey silt accumulation between April and August when compared to the silt and sandy silt concentrations that occurred between September and March. This was explained by the presence of 2 different type source regions of Africa, although the transport mechanism was similar. Similarly, clayey silt was the dominant sedimentary material of the riverine suspensions and no major differences in the data were obtained. Grain size distribution in the 3 marine core samples reflected the presence of a modern deltaic system, where sandy silt and silty sand sediments of the inner shelf graded to clayey silt of the delta front on the midshelf, and further offshore, clayey silt sediments occurred on the outer shelf to form prodeltaic deposits. Grain size changes within the cores were explained in terms the varying source, transportation, and depositional conditions over time. As a result of this research, the contribution of atmosphere and stream sediment inputs to the Cilician Basin budget was investigated. It was thought that the results obtained in this study will contribute significantly to the different research (sedimentological, mineralogical, geochemical, etc.) to be conducted in the Eastern Mediterranean.

**Key words:** Grain size, airborne dust, river-suspended, marine sediments, Mediterranean Sea

### 1. Introduction

In general, sediment particles are transported by a variety of mechanisms, such as wind, rivers, waves, glaciers, currents, and gravity mass movements, or in a combination of them (Hamann et al., 2008; Ehrmann et al., 2013; Cuadros et al., 2015; Ergin et al., 2018). Moreover, the distance from the source, types of source rocks, as well as the size, density, and shape of the grains also play an important role in defining the grain characteristics of the material transported and deposited in the environment (Shaw, 1978; Ergin et al., 2018). Nevertheless, speed, direction, height of the winds, intensity of rolling, jumping, saltation, and suspension effects may considerably determine the sedimentary texture of the materials deposited (Folk and Ward, 1957; Ashley, 1978; Bagnold and Barndorff-Nielsen, 1980) and sources. Thus, grain size distributions in sediments, based on various statistical parameters, have been widely used to determine the environmental factors of the basins (Sun et al., 2002). Coarse and fine grains (such as silt) in aeolian

dust are usually transported and deposited away from the source to surface storage areas by the surface winds and high level of air flow (Tsoar and Pye, 1987; Pye 1995).

The majority of the airborne dust stored in the drainage areas transported to the sea by coastal rivers, and also airborne dust stored directly in the marine environment, form the total airborne dust found in the sea bottom sediments. Such processes of fluvio-aeolian transportation processes may also control the grain size distribution and budget of the airborne dust in marine environments. There have been some studies on the storage (transport mechanisms and routes) and geochemical properties of airborne dust in the Netherlands (Reiff et al., 1986), North Atlantic (Prospero et al., 1987), Amazon Basin (Swap et al., 1992) and Black Sea (Kubilay et al., 1995). The Mediterranean basins are under the influence of dust from the deserts of North Africa (Sahara) and the Arabian Peninsula in the spring and summer (Martin et al., 1990; Dayan et al., 1991; Ganor, 1994; Kubilay and Saydam,

\* The author formerly worked at Institute of Marine Sciences, METU, Erdemli, Mersin, Turkey

\*\* Correspondence: vedat.ediger@tubitak.gov.tr

1995; Nickovic et al., 1997; Moulin et al., 1998; Krom et al., 1999). General geochemistry and mineralogy of airborne dust from the northeastern Mediterranean have been studied in detail within the framework of different purposes in some previous studies (Kubilay et al., 1994; Al-Momani, 1995; Kubilay et al., 1995; Guerzoni et al., 1997; Kubilay et al., 2000). As mentioned by McLaren (1981), the average grain size, modes, sorting, skewness, and kurtosis of the unconsolidated sediments are dependent on the distribution of the sediment grain size of its source, transportation, and sedimentary processes. Similar to the work performed by Torres-Padrón et al. (2002) in a different region, the grain size distribution of the airborne dust collected in this study was considered not only as a function of lateral transport distance, but also as a function of vertical transport.

The main objective of this study was, therefore, to analyze in detail the grain size distribution of the airborne dust that probably originated from the Arabian and the African deserts to the northeastern Mediterranean and compare it with that of riverine and marine sediments from sampling stations along the Erdemli coast of the Mersin Gulf, southeastern Turkey. In addition, the depositional rates and budgets of the sediments carried from 2 different basic regional sources (atmospheric and coastal rivers) were calculated. However, the significance of this study

was that the texture (grain size) characteristics have not been investigated in detail previously.

## 2. Study area

The study area is located on the western coast of the Mersin Bay, which is located at the northeastern corner of the Mediterranean Sea (Figure 1). The Mersin Bay is flanked on the northern/northwestern coastal hinterland by the high Taurus Mountains, which are composed mostly of Miocene limestones (Figure 1). However, a narrow stretch of ophiolitic rocks extend from west to east further inland. The study area is separated in the south from the continent of Africa by the eastern Mediterranean Sea and the Arabian Peninsula forms the southeastern boundary (Figures 1 and 2). In contrast to the high mountainous land topography in the north, the low topographic desert lands of Sahara/Africa are widely distributed in the south (Figures 1 and 2). Former studies on the synoptic meteorology of the region, air mass climatology, and the Erdemli Atmospheric Sampling Station have shown that the air flows from the Sahara and Arabian deserts (Figures 1 and 2) reached the region throughout the year, especially during the spring and autumn (Kubilay et al., 2000).

Since the Mediterranean Sea is a semiclosed basin, it is very sensitive to dust transportation and deposition due to its proximity to the deserts of North Africa

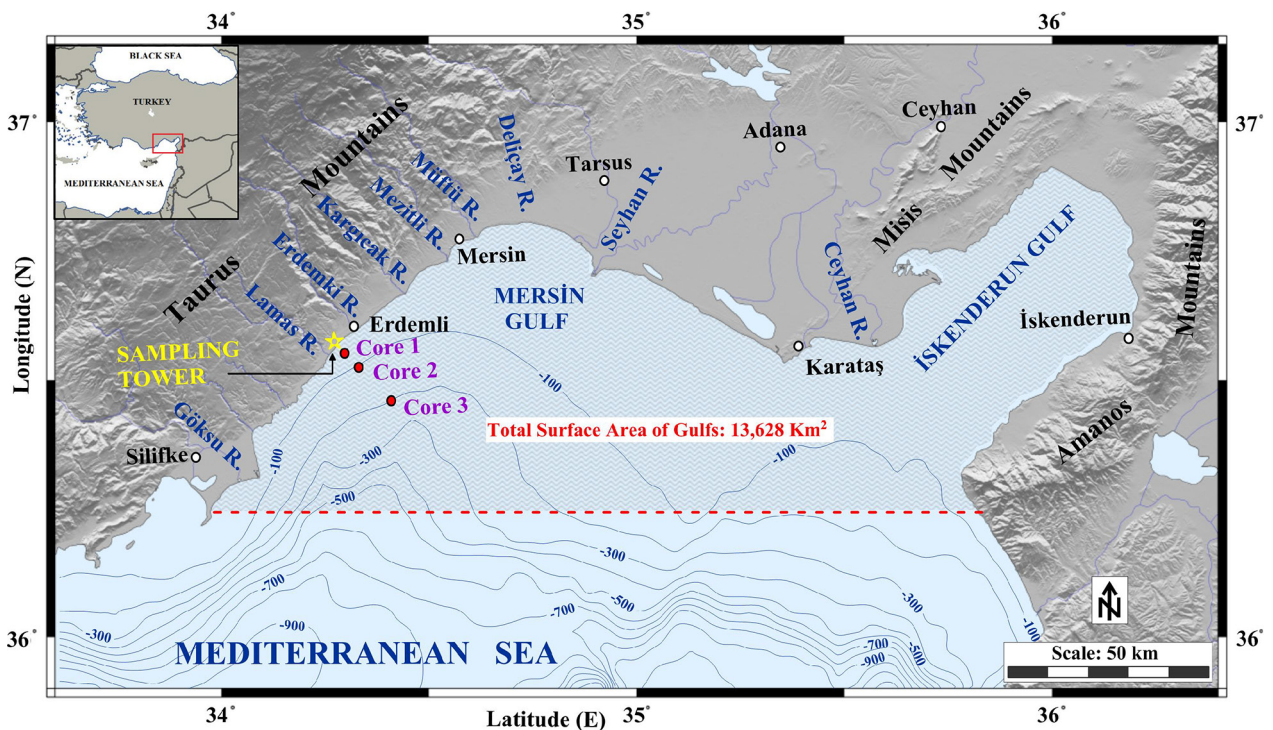


**Figure 1.** Index map of the study area showing the coastal mountains, atmosphere sampling station (yellow star), coastal rivers, coastal settlements, gulfs, total surface area of the gulfs (bounded by red dashed lines), and location of the gravity sediment cores. Water depths are given in meters.

(Sahara) and the Arabian Peninsula (Martin et al., 1990; Dayan et al., 1991; Ganor, 1994; Kubilay and Saydam, 1995; Ehrmann et al., 2013; Cuadros et al., 2015). It was reported that airborne dust was transported from the Middle East in the spring and from North Africa in the fall to the eastern Mediterranean (Dayan, 1986; Alpert et al., 1990). In the summer, airborne dust transport and deposits were found to be in the western Mediterranean (Moulin et al., 1998). Dust originating from the nearby deserts and the sediments carried by the coastal rivers are the most important sources of sea bottom sediments in the northeastern Mediterranean Sea.

The study area, Mersin Bay and thus the offshore waters of Erdemli, receive most of the sedimentary material deposited in the region from the northerly coastal rivers, which are of ephemeral nature (Figure 1 and Table 1). In addition, the easterly Tarsus and Seyhan Rivers may also contribute some quantities of sedimentary materials to the study area. It should be mentioned that sediment input from the southerly Nile River, along with major offshore currents (i.e. The POEM Group, 1992; Pinardi and Masetti, 2000; Hamann et al., 2008) transported towards the north and west, have also been reported previously. It was calculated that the total amount of sediment carried by the

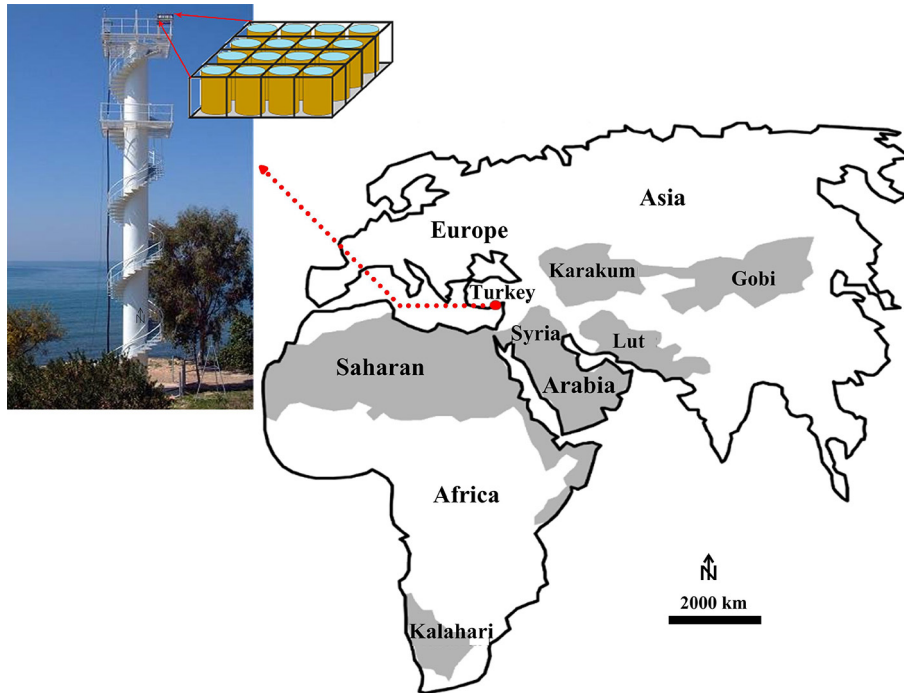


**Figure 2.** Map of the desert areas (in gray) in Africa, Arabia, and Asia. Red dot shows the location of the atmospheric sampling tower.

**Table 1.** Size of the drainage areas of the 5 different coastal rivers, average flow rates of the rivers, sediment loads, and annual sedimentation (Salihoğlu et al., 1987; Aksu et al., 1992; Özalp, 2009).

Rivers	Drainage area (km <sup>2</sup> )	Average flow rate (m <sup>3</sup> /s)	Sediment load (kg/s)	Annual sediment load (tons/year)
Ceyhan	20466	303	173.2	5462 × 10 <sup>3</sup>
Seyhan	19352	274	164.4	5185 × 10 <sup>3</sup>
Tarsus	1426	42	4.1	129 × 10 <sup>3</sup>
Lamas	1500	6	0.31	9846
Göksu	10065	126	80.5	2539 × 10 <sup>3</sup>
Total	52809	751	422.51	13 325 × 10 <sup>3</sup>

5 different continuous streams flowing to the northeastern Mediterranean region was  $13\,325 \times 10^3$  tons/year (Figure 1 and Table 1).

### 3. Materials and methods

#### 3.1. Sampling

##### 3.1.1. Airborne dust sampling

Samples of airborne dust (dry and wet) were collected from a 21-m-high atmospheric collection tower located on the Turkish Mediterranean coast in Erdemli ( $34^{\circ}15'18''$  E,  $36^{\circ}33'25''$  N) during 2001 (Figures 1 and 2). For the purpose of this research, a special sampler was designed for sampling of the total airborne dust during the annual time cycle. Dry and wet sampling sets, each consisting of 16 Teflon sample collection containers (depth of 25 cm and total surface area for each of 0.34212 m<sup>2</sup>, 0.32074 m<sup>2</sup>, or 0.25659 m<sup>2</sup>) were created to sample airborne dust entering the region. Later, airborne dust collected in the 16 collection containers of each set were then combined, dried, weighed, and collected in separate containers, and then used in the analysis. These samplers were then placed on top of the atmosphere sampling tower (Figures 1 and 2). Using these samplers, the airborne dust of the 1-year time period was sampled precisely. These samplers were capable of sampling vertically free-falling airborne dust (gravitationally settled), dust carried by winds, and dust in rain water (Levin and Ganor, 1996).

Samples were collected in 2001 to represent 7 different time periods (1st of February 2001 to 30th of January 2002, representing a 1-year time cycle; Table 2). During the sampling periods, the amount of airborne dust collected in the containers was checked from time to time and when it was observed that the amount of collected airborne dust reached a sufficient amount (>50 mg) for grain size analysis, that sampling was terminated and then sampling continued with a new sampling set. Thus, the 2001

sampling studies were completed with 7 different airborne dust samples representing different time intervals. In addition to the samples representing the 1-year period, wet and dry samples were also collected on 16 March 1998, 22 April 2001, 12 May 2001, 13 May 2001, and 14 May 2001, where high amounts of airborne dust reached the working area (Table 2). The sampling time intervals, total sampling days, total sample weights, and calculated daily sedimentation rates of the airborne dust are given in Table 2. Approximate daily storage rates were calculated using the time intervals and months corresponding to the dust in the airborne dust sampled (Table 2).

##### 3.1.2. Sampling of river-suspended loads

During a rainy period when the suspended loads of the coastal rivers increased (Göksu, Lamas, Erdemli, Kagicak, Mezitli, Müftü, and Deliçay; Figure 1), river waters were sampled using 15 L Teflon containers from place where the rivers met the sea and 1 m below the surface. River water samples in Teflon containers were dried under a fume hood at 60 °C, placed into sampling containers, weighed, and stored for grain size analyses and budget calculation.

##### 3.1.3. Marine sediment (core) sampling

Cores measuring 1 m long were collected using a gravity corer on board the R/V Lamas at sea water depths of 25 m (Core 1;  $34.29^{\circ}$  N,  $36.57^{\circ}$  E), 100 m (Core 2;  $34.33^{\circ}$  N,  $36.53^{\circ}$  E), and 200 m (Core 3;  $34.40^{\circ}$  N,  $36.46^{\circ}$  E) along a line that was perpendicular to the coast (Figure 1). After the cores were obtained, they were moved to the laboratory and then subsamples were taken from the cores for grain size analysis. A total of 10 subsamples, each 1 cm thick, were taken from each core for grain size analyses. Of the subsamples, 5 were taken from the top 5 cm of the cores (0–1 cm, 1–2 cm, 2–3 cm, 3–4 cm, and 4–5 cm) and the other 5 subsamples were taken at 10-cm-deep increments (10–11 cm, 20–21 cm, 30–31 cm, 40–41 cm, and 50–51 cm).

**Table 2.** Sampling time intervals, sampling days, total sampling weight, and daily sedimentation rates of the airborne dust samples.

Sampling time intervals	Total sampling days	Sampler surface area (m <sup>2</sup> )	Sample weight in the sampler (g)	Calculated total sample weight (g/m <sup>2</sup> )	Daily sedimentation (g/m <sup>2</sup> )
1 Feb. 2001–1 Apr. 2001	59	0.321	0.484	1.508	0.026
1 Apr. 2001–5 May 2001	34	0.342	1.164	3.401	0.1
5 May 2001–1 June 2001	27	0.342	1.739	5.082	0.188
1 June 2001–10 Sept. 2001	101	0.256	1.973	7.688	0.076
10 Sep. 2001–16 Oct. 2001	36	0.342	0.016	0.046	0.001
16 Oct. 2001–16 Nov. 2001	31	0.342	0.253	0.738	0.024
16 Nov. 2001–30 Jan. 2002	75	0.256	0.456	1.777	0.024
Total annual sedimentation rates (1 Feb. 2001–30 Jan. 2002)				20.25 g/m <sup>2</sup>	

### 3.2. Grain size analysis

Former studies of the eastern Mediterranean have reported that the grain size of the airborne dust ranged from 0.2 to 40  $\mu\text{m}$  (Dulac et al., 1992) and occasionally, the smallest grain length reached 0.15  $\mu\text{m}$  (Levin and Lindberg, 1979). Therefore, in this study, a Malvern Pananalytical Mastersizer 2000 laser particle sizer (Malvern, UK) was used to accurately measure the grain size of all of the sampled materials<sup>1</sup>. Sample material was passed through a laser beam resulting in the laser light being scattered at a wide range of angles. Detectors were used to measure the intensity of the light scattered at those positions. A mathematical model (Mie Theory) was applied to generate the particle size distribution. The final result was reported on an equivalent spherical diameter volume basis. This system was sensitive enough to measure grain sizes between 0.05 and 900  $\mu\text{m}$ , and provided measurements as a percentage of the volume occupied by certain grain sizes within the total sample volume. For the grain size distribution measurements of the airborne dust, river-suspended sediments, and subsamples of the marine sediment cores obtained in the study, the samples were suspended in distilled water and a few drops of ammonia were added. The purpose of adding the ammonia was to remove the flocculation effect in the sediments while the grain size measurements were being performed (Folk, 1974). Statistical parameters of the grain size distribution in Phi ( $\phi$ ) scale were calculated using the formula [ $\phi = -\log_2(\phi_{\text{mm}})$ ], as given by Folk and Ward (1957), and the results were presented.

### 3.3. Statistical analyses

Statistical analyses were performed on the results obtained from grain size analyses (Folk, 1974). The statistical values of the graphical parameters of the grain size distributions (mean, sorting, skewness, and kurtosis) contributed to the distinction between the different sedimentation environments and the understanding of the sediment transport processes. These calculated statistical parameters may provide insight into various aspects of the environmental, depositional, and transport conditions that the sediment grains endured, linking them to particular sedimentary systems.

Standard deviation is a precise measure of the scatter of grain size values from the mean, corresponding then to a measure of spread or sorting of the sample. In combination with the mean, the standard deviation is the most useful and widely applied value in granulometric statistics (Folk, 1974).

Skewness is used to establish the normality or symmetry of the distribution and hence to quantify the degree of dispersion within a sample, rather than only visualizing it on a frequency histogram. The closer the

skewness value is to zero, the more symmetrical (i.e. normal or unimodal) the distributions. Asymmetrical and multimodal sediment mixtures exhibit high values of skewness. The positive and negative sign of the skewness value indicates whether the asymmetrical tail extends to the left or right of the curve, as follows (Folk, 1974). Distribution curves highly skewed to low grain size values show a negative value and are diagnostic of environments with higher concentrations of silts and clays. The opposite are environments with higher concentrations of coarser materials, which show curves skewed to higher grain sizes and hence positive values. Kurtosis is also a quantitative measure to describe the degree of Gaussian normality of the grain size distribution, but in terms of how acute or flat the curve is. This is a sorting relation between the end members of the curve and its center (Folk, 1974). Both kurtosis and skewness values are ratios of dispersion; thus, they are dimensionless and do not have units.

## 4. Results

### 4.1. Grain size distribution of the airborne dust

A sample set representing a 1-year period was used to calculate the budget of airborne dust sampled at the Erdemli atmosphere station in 2001. However, grain size analysis was applied only to the samples of 4 different time periods and 5 different days, on which a sufficient amount of sample was collected for the grain size analyses (Table 2). Micrometer ( $\mu\text{m}$ ) scale grain size frequency distribution curves of the airborne dust samples are given in Figure 3a. The calculated statistical parameters of the grain size distributions of the airborne dust samples are given in Table 3.

When the grain size frequency distribution curves of each airborne dust sample drawn in the same graph and are examined, it is clearly seen that the frequency curves form 2 different groups (Figure 3a). Considering the sampling date periods of the airborne dust, it was concluded that the grain size distributions of the first group of samples were more clayey and represented transportation and deposition during the spring time (mainly between March and May). The more silty samples were deposited largely during the summer time (between May and September) (Figure 3b). Figure 3b also displays the total sand (S), silt (Z), and clay (C) percentages of all of the airborne dust samples on a triangular graph, where the airborne dust samples were classified according to the method of Folk and Ward (1957). Accordingly, the first group airborne dust samples can be considered as clayey silt, whereas second group samples may change from clayey-silt to silt (Figure 3b).

It seemed that the mean grain size of the airborne dust ranged from 6 to 8  $\phi$  and all of the dust samples were

<sup>1</sup> For detailed technical information, visit <https://www.malvernpanalytical.com/>

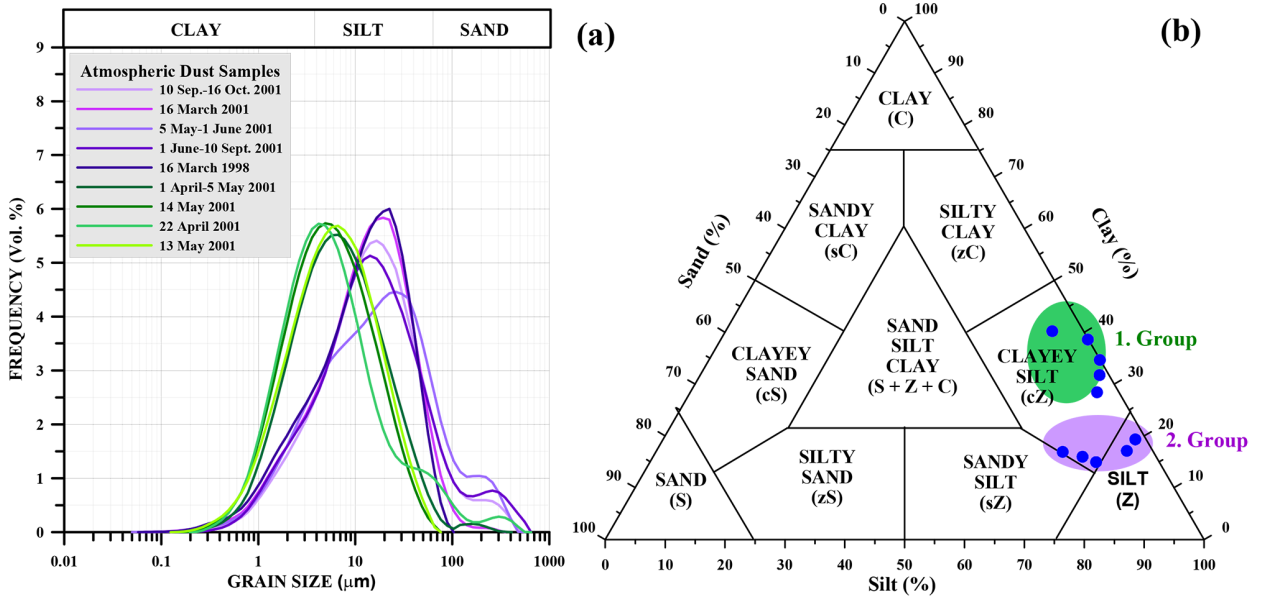


**Figure 3.** (a) Grain size frequency distribution of airborne dusts in  $\mu\text{m}$  scale. Green curves represent the spring samples (named as the 1st group) and purple curves represent the summer samples (named as the 2nd group). (b) Classification of the airborne dust samples in triangular graphs using the total sand, silt, and clay percentages.

**Table 3.** Statistical parameters of the grain size distribution of the airborne dust samples.

Sampling time	Mode 1 ( $\phi$ )	Mode 2 ( $\phi$ )	Mean ( $\phi$ )	Sorting (standard deviation)		Skewness ( $\phi$ )		Kurtosis ( $\phi$ )	
1 April–5 May 2001	7.237	2.610	7.355	-1.538	VWS	0.009	S	0.961	MK
5 May–1 June 2001	5.254	2.389	6.143	-2.014	VWS	-0.053	S	1.001	MK
1 June–10 Sept. 2001	6.135	1.949	6.272	-1.923	VWS	0.008	S	1.143	LK
10 Sept.–16 Oct. 2001	5.915	2.169	6.274	-1.772	VWS	-0.051	S	1.093	MK
16 March 1998 (wet)	5.474		6.639	-1.621	VWS	-0.234	CS	0.968	MK
16 March 1998 (dry)	5.694		6.502	-1.624	VWS	-0.187	CS	1.015	MK
22 April 2001	7.898	1.728	7.610	-1.725	VWS	0.169	FS	1.144	LK
12 May 2001	6.796	2.169	7.045	-1.764	VWS	-0.041	S	0.901	MK
13 May 2001	7.237		7.532	-1.493	VWS	-0.045	S	0.959	MK
14 May 2001	7.677		7.669	-1.461	VWS	-0.001	S	0.948	MK

VWS: very well sorted, S: skewed, CS: course skewed, FS: fine skewed, MK: mesokurtic, LK: leptokurtic.

very well sorted (VWS) and it was also apparent that all of the airborne dust samples had widespread symmetric (S) and mesokurtic (MK) distribution (Table 3). In general, the airborne dust samples showed bimodal distribution (Figure 3a and Table 3). When the average grain size frequency distribution curves and statistical values of the airborne dust samples were examined, the grain size distribution showed the existence of 2 different groups (Figure 3a).

The mean values of the grain size distribution data (Figure 3a), which constitute the frequency curves of

each group, were calculated and the grain size frequency distribution curves of each group were prepared (Figure 4a). It was concluded that this grouping could have been caused by airborne dust originating from 2 different atmospheric conditions and/or 2 different sources.

The grain size frequency distribution curves of the airborne dust samples collected under wet and dry weather conditions on 16 March 1998, which traveled along the line given in the satellite images, are also given in Figure 4b. When the graphics given in Figure 4b were examined, it was concluded that the grain size frequency distributions

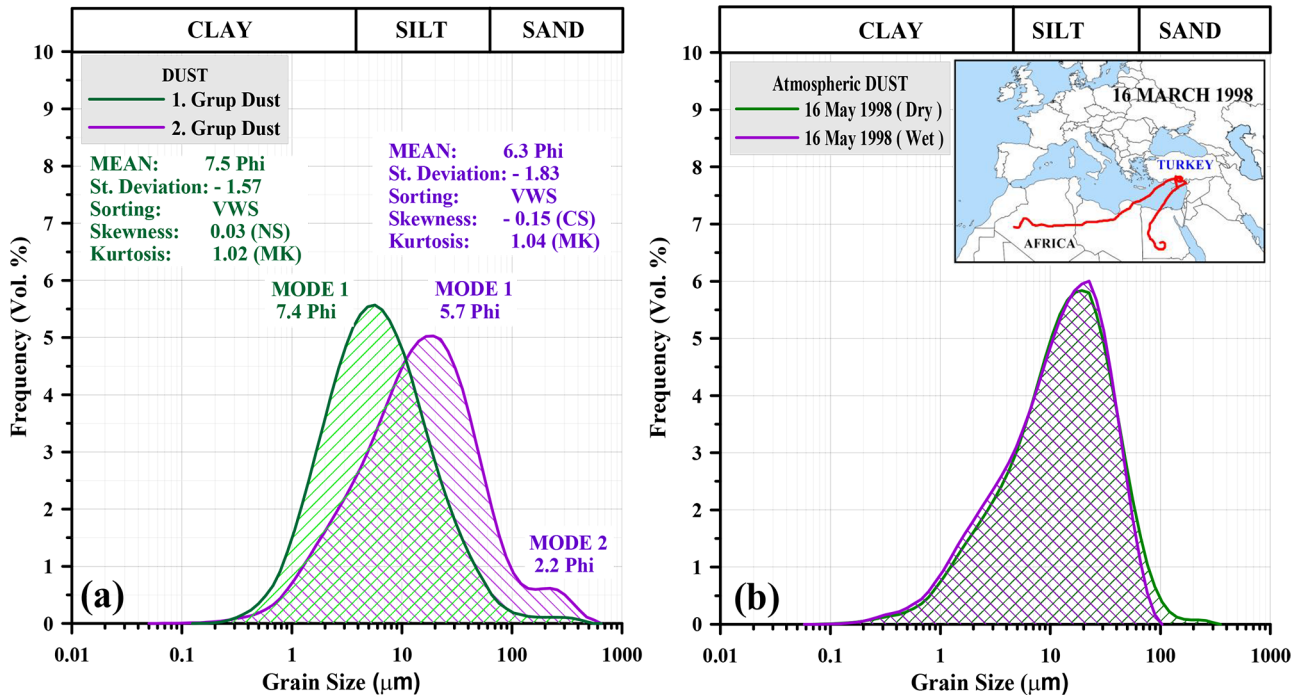


**Figure 4.** (a) Average grain size frequency distribution and statistical data for each group. (b) Grain size frequency distribution of the airborne dust collected on 16 March 1998, under wet and dry weather conditions.

of the deposits that accumulated under both wet and dry conditions on the same day had similar characteristics.

The grain size frequency distributions of the airborne dust samples of 3 consecutive days (12, 13, and 14 May 2001) were superimposed on the graph in Figure 5. Examination of the values in Table 3 suggested that the first modes of the airborne dust deposited on 12, 13, and 14 May 2001 were  $6.8 \phi$ ,  $7.2 \phi$ , and  $7.7 \phi$ , and the mean grain sizes were  $7.0 \phi$ ,  $7.5 \phi$ , and  $7.7 \phi$ , respectively. From the data, it can be inferred that the grain size of the airborne dust decreased over time depending on the settling velocities (Figure 5). Given the fact that coarse grains will be settled faster than fine grains, the reason why the average grain size of the airborne dust on these 3 consecutive days decreased over time was easily understood. The reason why the amount of coarse silt and fine sand deposited on 12 May 2001 was higher than the airborne dust deposited on 13 and 14 May 2001 (Figure 5) can easily be understood by considering Stokes' law.

Daily deposition rates of the airborne dust for each month were calculated and presented as a bar graph (Table 2 and Figure 6). When Figure 6 was examined, it was observed that the daily sedimentation rates generally had high values between April and August. However, it was concluded that the highest daily storage rate was in May.

#### 4.2. Grain size distribution of the river-suspended loads

The suspended load samples obtained from the 7 main rivers (Figure 1) flowing into the basin were included in

the project with other data in the archive, and their grain size distributions are presented in Figure 7.

The grain size frequency distributions of the suspended loads of these samples (Figure 7a), when transferred to a triangular graph, with the exception of the more silty Göksu River suspensions, can be classified according to the method of Folk and Ward (1957) as clayey silt (Figure 7b).

Statistical analysis on grain size distribution displayed a single mode that ranged between  $6$  and  $8 \phi$ . The mean grain size distribution of all of the samples was around  $8 \phi$  (Table 4). River-suspended sediments, which fell within a narrow size range, were calculated as VWS and they mostly fell within the S and MK classes (Folk, 1974 classification; Table 4).

#### 4.3. Grain size distribution of marine sediments

The grain size analyses were performed on ten 1-cm-thick subsamples taken along the sediment cores. Frequency distribution curves of the grain size data obtained along the core subsamples were plotted and are given in Figures 8a–8c.

With the exception of core 3, the 2 other cores, 1 and 2, displayed bimodal frequency distribution curves (Figure 8a–8c). It was found that in core 1, the first mode was within the range of  $3$ – $4 \phi$  and the presence of the 2nd mode was observed below the 20 cm depth of core 1, with values around  $6.6 \phi$  (Table 5). In core 2, the first mode existed at about  $7 \phi$ , while mode 2 occurred at nearly  $2 \phi$  above the 5-cm core depths. Despite this, only the 1st mode had

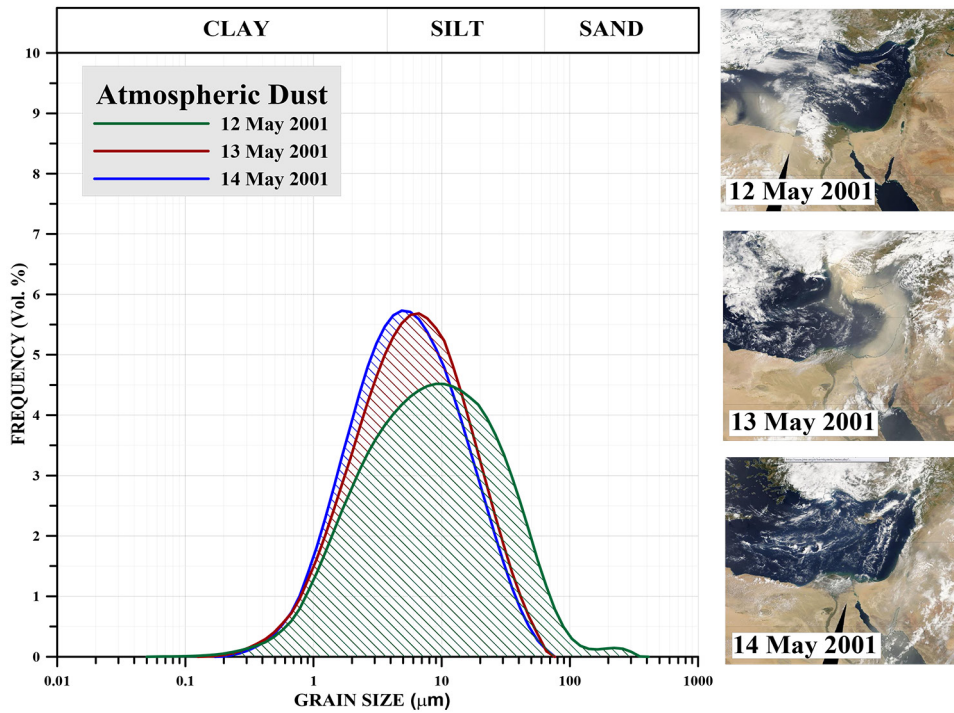


**Figure 5.** Grain size frequency distributions of the airborne dust samples collected on 3 consecutive days (12, 13, and 14 May 2001). Satellite images showing the possible sources and transport pathways of the airborne dust deposited on these days. Red dot represents the location of the sampling station.

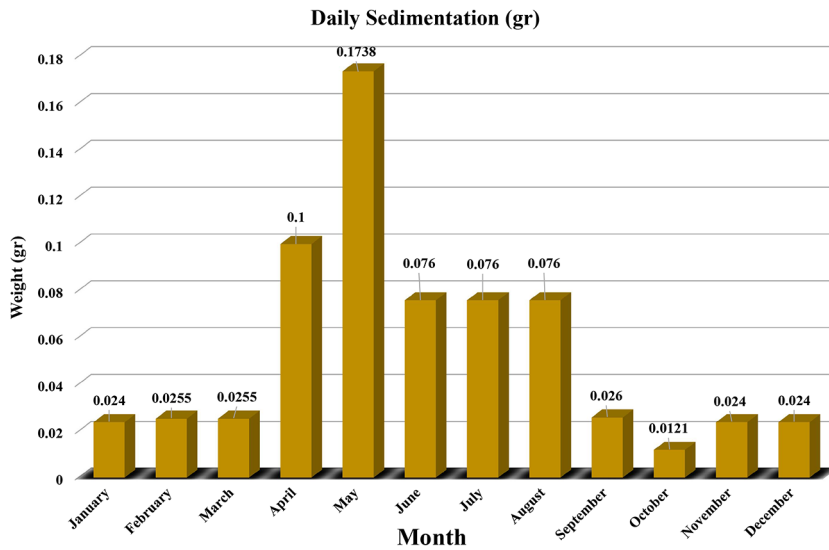


**Figure 6.** Bar graph showing the daily deposition rate of the airborne dust corresponding to each month.

values around  $7 \phi$ , and no 2nd mode was observed along core 3 (Table 5).

The results of the statistical analysis on the cumulative distributions (in  $\phi$  scale) are also presented in Table 6. As shown, the mean grain size of all of the subsamples along core 1 was between 4 and 5  $\phi$ . The mean grain size of all of

the subsamples along core 2 ranged between 5 and 7.6  $\phi$ , and the values from core 3 were around 7  $\phi$ . Accordingly, the sediments of core 1 and core 2 displayed VWS, leptokurtic (LK), and MK distribution of the grains (Table 6). The grains of the sediments along core 3 were VWS, S, and MK (Table 6).

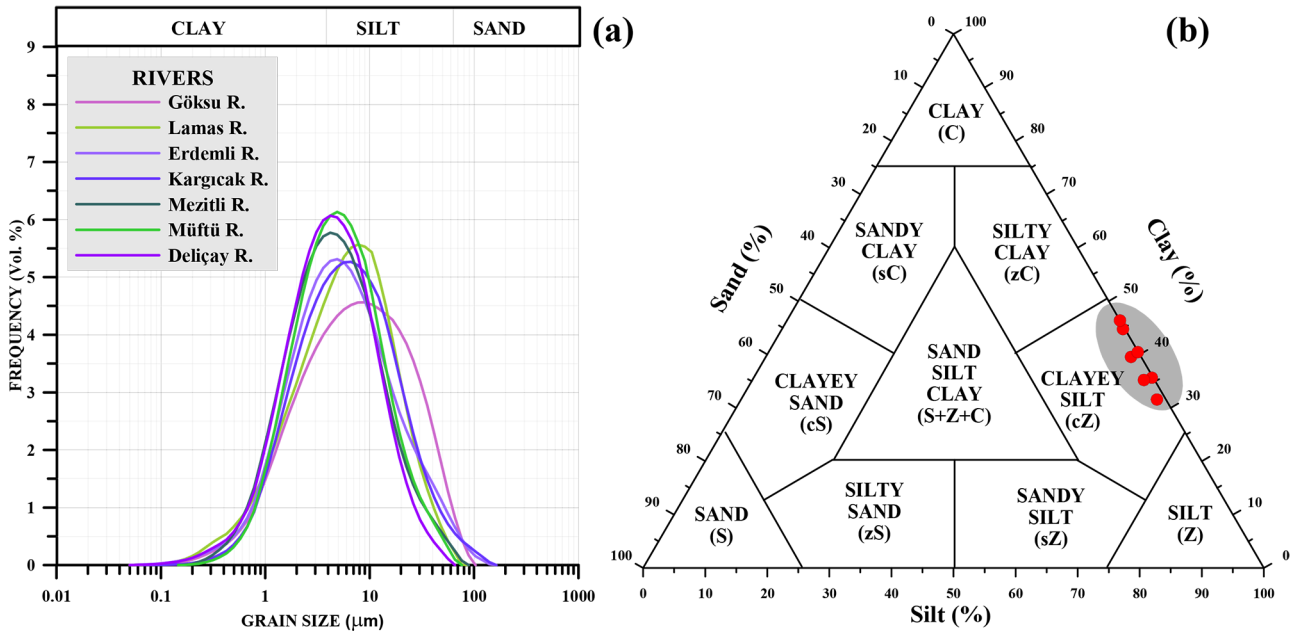


**Figure 7.** (a) Grain size frequency distribution ( $\mu\text{m}$  scale) of the suspended loads carried by coastal rivers flowing into Mersin Bay. (b) Classification of the suspended loads of the coastal rivers in a triangular graph using the total sand, silt, and clay percentages.

**Table 4.** Statistical results of the grain size distributions of the suspended river load samples.

River	Mode ( $\phi$ )	Mean ( $\phi$ )	Sorting (standard deviation)		Skewness		Kurtosis	
Göksu	6.796	7.237	-1.747	VWS	-0.062	S	0.900	MK
Lamas	7.016	7.600	-1.604	VWS	-0.118	CS	0.993	MK
Erdemli	7.677	7.632	-1.659	VWS	0.047	S	1.003	MK
Kargıcak	7.237	7.492	-1.578	VWS	0.001	S	0.958	MK
Mezitli	7.898	7.903	-1.483	VWS	0.024	S	0.986	MK
Muftu	7.677	7.767	-1.389	VWS	0.010	S	0.981	MK
Deliçay	7.898	8.001	-1.409	VWS	-0.027	S	0.991	MK

VWS: very well sorted, S: symmetrical, CS: coarse symmetrical, and MK: mesokurtic.

Total sand, silt, and clay percentages of the sediment samples obtained from cores 1, 2, and 3 were transferred to triangular graphs and classified according to the method of Folk and Ward (1957) (Figures 8d–8f). The inner shelf sediments of core 1 were both of silty sand (zS) and sandy silt (sZ) (Figure 8d), whereas the midshelf sediments of core 2 were clayey-silt (cZ), with the exception of 1 sample (sand-silt-clay; SZC) (Figure 8e). The outer shelf sediments of core 3 were predominantly clayey silt (cZ) (Figure 8f).

## 5. Discussion and conclusions

### 5.1. Grain size distribution in airborne dusts

The frequency distribution curves of the airborne dust

samples given in Figure 3 indicated the presence of at least 2 different groups. The airborne dust samples from the spring (between 5 May and 1 June 2001) represented the 1st group of clayey deposits and the airborne dust samples corresponding to the summer (between 1 June and 10 September 2001) represented the 2nd group of silty deposits (Figure 3). In addition, the statistical parameters of each group of airborne dust samples are given in Figure 4.

The airborne dust samples from the summer that had 2 modes (5.7 and 2.2  $\phi$ ) were found to be coarser-grained than the spring airborne dust samples that had a single mode (7.4  $\phi$ ) (Figure 4a). The coarse grains observed in small quantities in the total sediment should

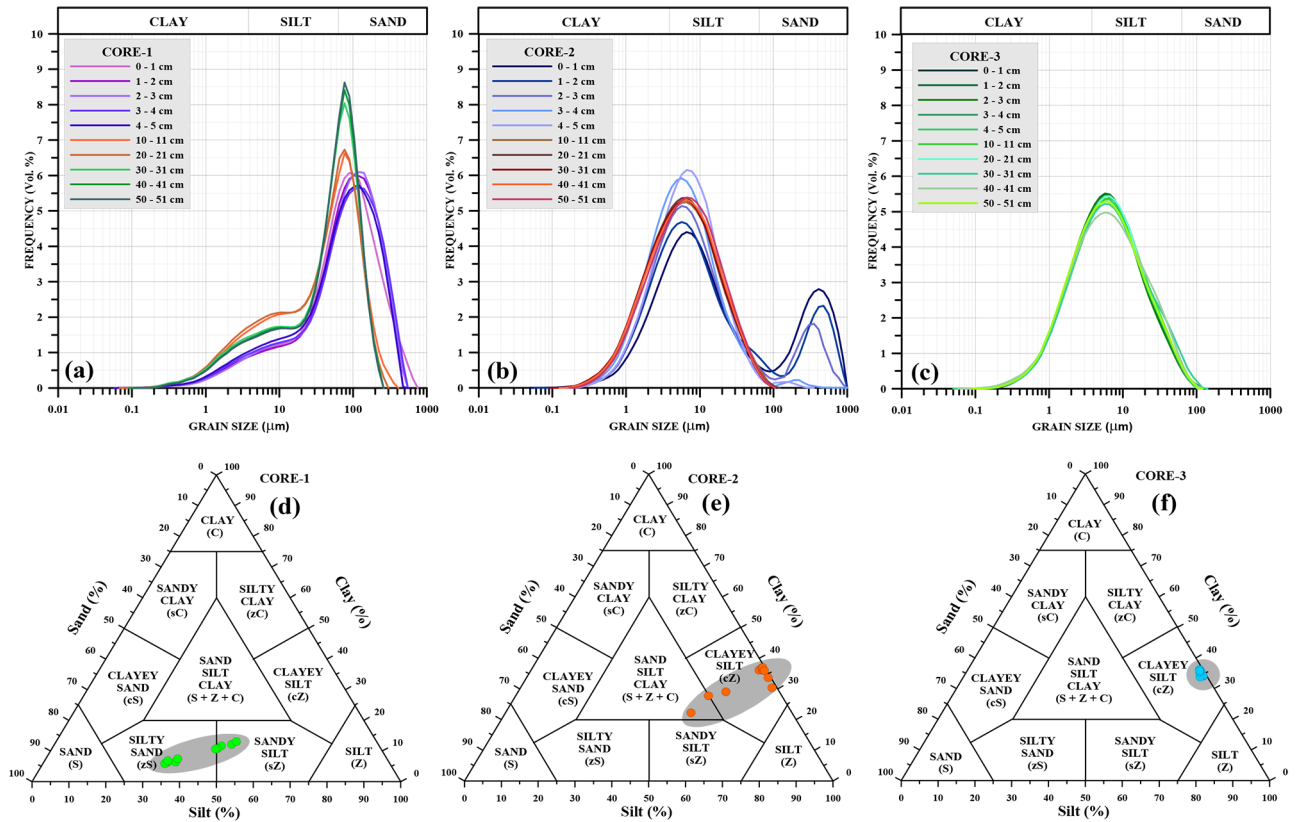


**Figure 8.** (a–c) Grain size frequency distribution (µm scale) of the subsamples obtained along the 3 different sediment cores taken from Mersin Bay (see for location; Figure 1). (d–f) Classification of the subsamples in triangular graphs on the basis of the total sand, silt, and clay percentages.

**Table 5.** Calculated grain size modes along the cores studied.

Core intervals (cm)	Core 1		Core 2		Core 3
	Mode 1 Phi (φ)	Mode 2 Phi (φ)	Mode 1 Phi (φ)	Mode 2 Phi (φ)	Mode 1 Phi (φ)
0–1	3.491		7.237	1.288	7.457
1–2	3.271		7.457	1.067	7.457
2–3	3.05		7.457	1.508	7.457
3–4	3.05		7.457	2.169	7.237
4–5	3.05		7.237	2.830	7.457
10–11	3.711		7.237		7.237
20–21	3.711	6.576	7.237		7.237
30–31	3.711	6.576	7.237		7.457
40–41	3.711	6.576	7.237		7.457
50–51	3.711	6.576	7.237		7.457

generally have probably originated from regional sources. As a possible cause of these seasonal variations in the grain sizes may have been due to changing provenance and atmospheric conditions in the spring and summer (Figure 3). Moreover, on the basis of the satellite photos,

it was suggested that fine-grained (mode 1) airborne dust must have accumulated in the spring and may have been transported from a distant source (Sahara) and was stored under low-energy atmospheric conditions (SW or SSW). The average frequency curve of the airborne dust from the

**Table 6.** Statistical results of the grain size distribution of core subsamples.

Subsamples (cm)		0–1	1–2	2–3	3–4	4–5	10–11	20–21	30–31	40–41	50–51
Core 1 (inner shelf)	Mean Phi ( $\phi$ )	4.193	4.119	4.104	4.16	4.315	5.177	5.271	5.087	5.018	4.995
	Standard deviation (sorting)	–1.974	–1.933	–1.944	–2.05	–2.062	–2.081	–2.079	–2.009	–1.958	–1.942
		VWS									
	Skewness (symmetricity)	–0.323	–0.369	–0.375	–0.372	–0.379	–0.417	–0.433	–0.512	–0.519	–0.527
		VCS									
	Kurtosis	1.258	1.217	1.181	1.149	1.11	0.903	0.871	0.979	1.013	1.025
LK		LK	LK	LK	LK	MK	PK	MK	MK	MK	
Core 2 (midshelf)	Mean Phi ( $\phi$ )	5.654	6.101	6.852	7.58	7.394	7.531	7.582	7.585	7.541	7.448
	Standard deviation (sorting)	–3.011	–2.91	–2.317	–1.511	–1.441	–1.613	–1.592	–1.607	–1.6	–1.582
		VWS									
	Skewness (symmetricity)	0.379	0.407	0.304	0.024	–0.03	–0.017	–0.023	–0.035	–0.038	–0.04
		VFS	VFS	VFS	S	S	S	S	S	S	S
	Kurtosis	0.744	1.135	1.325	1.035	1.01	0.958	0.966	0.962	0.956	0.958
PK		LK	LK	MK							
Core 3 (outer shelf)	Mean Phi ( $\phi$ )	7.497	7.476	7.553	7.503	7.514	7.451	7.455	7.381	7.443	7.5
	Standard deviation (sorting)	–1.595	–1.598	–1.596	–1.603	–1.634	–1.621	–1.607	–1.672	–1.697	–1.626
		VWS									
	Skewness (symmetricity)	0.006	0.008	–0.01	–0.012	–0.012	–0.019	–0.008	0.027	–0.001	0.005
		S	S	S	S	S	S	S	S	S	S
	Kurtosis	0.986	0.991	0.991	0.987	0.99	0.986	0.988	0.973	0.946	0.971
MK		MK									

VWS: very well sorted, VCS: very coarse symmetrical, LS: leptokurtic, and MK: mesokurtic.

2nd group showed that the curve had 2 modes. Likewise, as reported from Offshore Cape Blanc (Karakas et al., 2006), the coarser-grained airborne dust materials caused a 2nd mode (2.2  $\phi$ , Figure 4a) frequency curve, as an indication of different regional sources. Thus, the summer samples were characterized by a weaker sorting than the spring airborne dust samples (Figure 4a).

In addition, similar results of the grain size frequency distributions of airborne dust were also found under both wet and dry conditions on 16 March 1998 (Figure 4b). This would also lead to the assumption that the airborne dust must have been carried with no dependence on storage under wet or dry weather conditions. A back trajectory figure is given at the top of Figure 4b, suggesting that the airborne dust reaching the region on 16 March 1998 originated from the Sahara Desert (North Africa).

When the satellite image of 12 May 2001 was examined, it was seen that coarse-grained airborne dust originating from the Sahara Desert reached the

sampling station from the SW. On the other hand, fine-grained airborne dust originating from Arabia reached the sampling station from the S on 13 and 14 May 2001. Obviously, at proximal locations (where airborne dust was deposited relatively close to its source), the particles were coarser-grained and mass accumulation rates were larger than at more distal locations (where airborne dust was deposited relatively far from its source). This observation was first prominently described by Sarnthein et al. (1981) from NW Africa. As a result, it can also be concluded that the textural characteristics (VWS, S, and MK) from these successive days showed some similarities. The role of airborne dust of African-Arabian origin in contributing fine-grained sediment to the eastern Mediterranean and thus to the studied Mersin Bay area was also reported by Chester et al. (1977), Ganor and Mamane (1982), and Hamann et al. (2008).

**5.2. Grain size distribution in the river-suspended loads**  
The grain size distribution of the river-suspended

sediments transported to the Mersin Bay by coastal rivers showed a single mode distribution between 6.8 and 7.9  $\phi$ . In addition, the grain size distributions of all river-suspended sediments displayed VWS, S, and MK materials (Figure 7, Table 4). It was clear that the grain size distributions of the airborne dust in the spring months (Figure 4) had similar sorting, skewness, and kurtosis values to those of the river-suspended loads, considering that the airborne dust stored in the river-drainage areas would have been, or may have been in part, transported to Mersin Bay by the rivers during the rainy spring season. Based on former studies from or close to the study area (Shaw, 1978; Mange-Rajetzky, 1983; Ergin et al., 1992; Ediger et al., 1997; Okyar et al., 2005; Ehrmann et al., 2007), it can be concluded that most of the sedimentary material deposited on the sea floor off of the Lamas River mouth must have originated from weathering of the rocks of the coastal hinterland and been transported to the sea by coastal rivers (Göksu, Tarsus, and Seyhan rivers from western and eastern sectors of Mersin Bay). It is also likely, even of lesser importance or at least in part, that the Nile River (Shaw, 1978; Ehrmann et al., 2007; Hamann et al., 2008) from the southeastern Mediterranean area together with the prevailing current system (The POEM Group, 1992; Pinardi and Masetti, 2000) could have contributed fine sediment to the studied area.

### 5.3. Grain size distribution in the sediment cores

When the grain size frequency curves of the marine sediments obtained from the 3 different water depths of the Mersin Bay shelf were examined (Figure 8), it seemed that the sediments displayed decreasing grain sizes with increasing distance from the Lamas River mouth, where a shallow to deep deltaic depositional system likely occurred. The sediments of core 1, taken from a water depth of 25 m (representing the inner shelf), had a bimodal, heterogeneous, and slightly coarser-grained texture (silty sand to sandy silt), where the proximity to the sediment input was of greater importance. On the other hand, the sediments of core 2, taken from a water depth of 100 m (representing the midshelf), were marked by a bimodal and partly homogeneous grain size (sand-silt-clay to clayey silt). The sediments of core 3, obtained from a water depth of 200 m (representing the outer shelf), had a single mode and completely homogeneous grain size (clayey silt). Such grain size grades from sand and silt near the shore to silty clay further out offshore could have been indicative of the formation of a modern delta (Lewis, 1984; Ergin et al., 1998; Palinkas and Nittrouer, 2007), which now appeared to be present off the Lamas River mouth. The high percentage of sandy grains along in core 1 must have been the result of the coastal wash effects (Elfrink and Baldock, 2002) by strong waves and currents alone, or in combination with materials from the strong floods after heavy rainfalls. The presence

of fine-grained sands within the upper 5 cm section of the core 2 was more likely due to the combination of processes derived from the marine and land-based sources (i.e. currents, river input, and bottom mass movements). The grain size of the sea bottom sediments from the inner shelf to the midshelf and from there to the outer shelf decreased inversely with the water depth along the direction of the red arrow shown in Figure 9.

### 5.4. Sedimentation rate of the airborne dust

As shown in Table 2, it was evident that the desert-based airborne dust reaching the Erdemli Atmospheric Sampling Station reached its highest daily storage rate in May (spring) (Figure 6). In the case of the atmospheric synoptic inversion work in 2001, it was thought that the interpretations made on the subject may become definite. The daily deposition amount of the airborne dust varied between its highest value in May (0.19 g/m<sup>2</sup> per day) and its 2nd highest value in April (0.1 g/m<sup>2</sup> per day).

Between 1 February 2001 and 30 January 2002, the total annual amount of airborne dust deposited in the region was calculated as 20.25 g/m<sup>2</sup>/year. The total surface area of Mersin Bay and İskenderun Gulf was calculated as 13,628 km<sup>2</sup> (Figure 1). Thus, in a 1-year storage period, it was estimated that approximately 275,967 tons/year of dust were deposited directly from the atmosphere to the limited marine area (Table 2, Figures 1 and 9). It was concluded that the total amount of sediment carried by the 5 different continuous rivers flowing to the northeastern

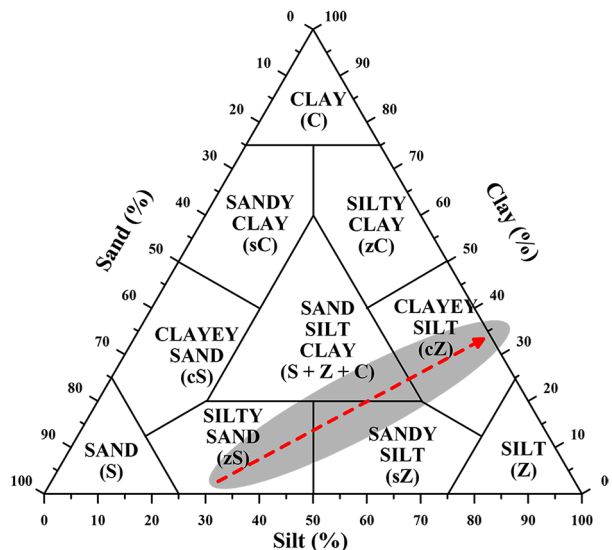


**Figure 9.** Classification of all of the subsamples collected along the cores (1, 2, and 3) in a triangular graph using the total sand, silt, and clay percentages. The direction of the red arrow drawn on the triangle grain size classification graphic clearly shows that the grain size of the bottom sediments decreased despite the increase in water depth.

Mediterranean Region was 13,325,000 tons/year (Table 1). Thus, it was calculated that the amount of annual deposition of both river-suspended sediments (13,325,000 tons/year) and airborne dust (275,967 tons/year) in the limited area (Figure 1) was 13,600,967 tons/year.

It is a fact that the total amount of sediment (Figure 1) carried by the coastal rivers to the Mersin and İskenderun basins also includes airborne dust accumulated in the drainage areas of the coastal rivers (calculated value of 1,069,382 tons/year). For this reason, it should be taken into account that the amount of airborne dust annually deposited in the marine environment limited area in Figure 1 should be higher than the calculated value.

## References

- Aksu AE, Uluğ A, Piper DJ - W, Konuk YT, Turgut S (1992). Quaternary Sedimentary History of Adana, Cilicia and İskenderun Basins: Northeast Mediterranean Sea. *Marine Geology* 104: 55-71. doi: 10.1016/0025-3227(92)90084-U
- Al-Momani IF (1995). Long-range atmospheric transport of pollutants to the eastern Mediterranean basin. PhD, METU, Ankara, Turkey.
- Alpert P, Neeman BU, Shay-El Y (1990). Intermonthly variability of cyclone tracks in the Mediterranean. *Journal of Climate*: 3: 1474-1478. doi: 10.1175/1520-0442(1990)003<1474:IVOCTI>2.0.CO;2
- Ashley GM (1978). Interpretation of polymodal sediments. *Journal of Geology* 86: 411-421.
- Bagnold RA, Barndorff-Nielsen O (1980). The pattern of natural size distributions. *Sedimentology* 27: 199-207. doi: 10.1111/j.1365-3091.1980.tb01170.x
- Chester R, Baxter GG, Behairy AKA, Connor K, Cross D et al. (1977). Soil-sized eolian dusts from the lower troposphere of the eastern Mediterranean Sea. *Marine Geology Volume 24, Issue 3*: 201-217. doi: 10.1016/0025-3227(77)90028-7
- Cuadros J, Diaz-Hernandez JI, Sanchez-Navas A, Garcia-Casco A (2015). Role of clay minerals in the formation of atmospheric aggregates of Saharan dust. *Atmospheric Environment* 120: 160-172. doi: 10.1016/j.atmosenv.2015.08.077
- Dayan U (1986). Climatology of back trajectories from Israel based on synoptic analysis. *Journal of Climate and Applied Meteorology* 25 (5): 591-595. doi: 10.1175/1520-0450(1986)025<0591:COBTFI>2.0.CO;2
- Dayan U, Heffter J, Miller J, Gutman G (1991). Dust intrusion events into the Mediterranean basin. *Journal of Applied Meteorology* 30: 1185-1199. doi: 10.1175/1520-0450(1991)030<1185:DIEITM>2.0.CO;2
- Dulac F, Tanre D, Bergametti G, Buat-Menard P, Desbois M et al. (1992). Assessment of the African airborne dust mass over the western Mediterranean Sea using Meteosat data. *Journal of Geophysical Research: Atmospheres* 97: 2489-2506. doi: 10.1029/91JD02427
- Ediger V, Evans G, Ergin M (1997). Recent surficial shelf sediments of the Cilician Basin (Turkey), northeastern Mediterranean. *Continental Shelf Research* 17 (13): 1659-1677. doi: 10.1016/S0278-4343(97)00030-7
- Ehrmann W, Schmiedl G, Hamann Y, Kuhnt T, Hemleben C et al. (2007). Clay minerals in late glacial and Holocene sediments of the northern and southern Aegean Sea. *Palaeogeography, Palaeoclimatology, Palaeoecology* 249: 36-57. doi: 10.1016/j.palaeo.2007.01.004
- Ehrmann W, Seidel M, Schmiedl G (2013). Dynamics of Late Quaternary North African humid periods documented in the clay mineral record of central Aegean Sea sediments. *Global and Planetary Change* 107: 186-195. doi: 10.1016/j.gloplacha.2013.05.010
- Elfrink B, Baldock T (2002). Hydrodynamics and sediment transport in the swash zone: a review and perspectives. *Coastal Engineering Issues*; 3-4, 45: 149-167. doi: 10.1016/S0378-3839(02)00032-7
- Ergin M, Karakaş ZS, Tekin E, Eser B, Sözeri K et al. (2018). Provenance discrimination among foreshore, backshore, and dune environments in the black sand beaches along the Samandağ/Hatay coasts, SE Turkey (E Mediterranean). *Arabian Journal of Geosciences* 11: 109. doi: 10.1007/s12517-018-3429-2.
- Ergin M, Kazan B, Yücesoy F, Okyar M (1998). Hydrographic, Deltaic and Benthogenic Controls of Sediment Dispersal in the Gulf of İskenderun, SE Turkey (E. Mediterranean). *Estuarine Coastal and Shelf Science* 46: 493-502. doi: 10.1006/ecss.1996.0231
- Ergin M, Okyar M, Timur K (1992). Seismic stratigraphy and late quaternary sediments in inner and mid-shelf areas of eastern Mersin Bay, northeastern Mediterranean Sea. *Marine Geology* 104 (1-4): 73-91. doi: 10.1016/0025-3227(92)90085-V
- Folk RL, Ward WC (1957). Brazos River bar, a study in the significance of grain size parameters. *Journal of Sedimentary Petrology* 27: 3-26. doi: 10.1306/74D70646-2B21-11D7-8648000102C1865D
- Folk RL (1974). *Petrology of Sedimentary Rocks*. Hemphill Publishing Co., Austin, p. 170. <http://hdl.handle.net/2152/22930>

- Ganor E (1994). The frequency of Saharan dust episodes over Tel Aviv, Israel. *Atmospheric Environment* 28 (17): 2867-2871. doi: 10.1016/1352-2310(94)90087-6
- Ganor E, Mamane Y (1982). Transport of Saharan dust across the eastern Mediterranean, in *Atmospheric Environment* 16 (3): 581-587. doi: 10.1016/0004-6981(82)90167-6
- Guerzoni S, Molinaroli E, Chester R (1997). Saharan dust inputs to the western Mediterranean Sea: depositional patterns, geochemistry and sedimentological implications. *Deep-Sea Research Part II* 44 (3-4): 631-654. doi: 10.1016/S0967-0645(96)00096-3
- Hamann Y, Ehrmann W, Schmiel G, Krüger S, Stuetz JB et al. (2008). Sedimentation processes in the eastern Mediterranean Sea during the Late Glacial and Holocene revealed by end-member modelling of the terrigenous fraction in marine sediments. *Marine Geology* 248: 97-114. doi: 10.1016/j.margeo.2007.10.009
- Karakaş G, Nowald N, Blaas M, Marchesiello P, Frickenhaus S et al. (2006). High-resolution modeling of sediment erosion and particle transport across the northwest African shelf. *Journal of Geophysical Research* 111: 0148-0227. doi: 10.1029/2005JC003296
- Krom MD, Cliff RA, Eijssink LM, Herut B, Chester R (1999). The characterization of Saharan dusts and Nile particulate matter in surface sediments from Levantine Basin using Sr isotopes. *Marine Geology* 155: 319-330. doi: 10.1016/S0025-3227(98)00130-3
- Kubilay N, Slobodan N, Cyril M, Dulac F (2000). An illustration of the transport and deposition of mineral dust onto the eastern Mediterranean. *Atmospheric Environment* 34: 1293-1303. doi: 10.1016/S1352-2310(99)00179-X
- Kubilay N, Yemenicioğlu S, Saydam AC (1994). Trace metal characterization of airborne particles from the northeastern Mediterranean. *Fresenius Environment Bulletin* 3 (7): 444-448.
- Kubilay N, Yemenicioğlu S, Saydam AC (1995). Airborne material collections and their chemical composition over the Black Sea. *Marine Pollution Bulletin* 30 (7): 475-483. doi: 10.1016/0025-326X(95)00238-I
- Kubilay N, Saydam AC (1995). Trace elements in atmospheric particulates over the Eastern Mediterranean; concentrations, sources, and temporal variability. *Atmospheric Environment* 29 (17): 2289-2300. doi: 10.1016/1352-2310(95)00101-4
- Levin Z, Ganor E (1996). The effects of desert particles on cloud and rain formation in the eastern Mediterranean. In: Guerzoni, S, Chester, R (Eds.), *The Impact of African Dust Across the Mediterranean*. Kluwer Academic Publishers, Norwell, MA, pp. 77-86.
- Levin Z, Lindberg JD (1979). Size distribution, chemical composition and optical properties of urban aerosols in Israel. *Journal of Geophysical Research* 84: 6941-6950. doi: 10.1029/JC084iC11p06941
- Lewis DW (1984). *Practical Sedimentology*, Hutchinson Ross Publishing Company, New York, p. 227.
- Mange-Rajetzky MA (1983). Sediment dispersal from source to shelf on an active continental margin, S. Turket, *Marine Geology* 52: 1-26. doi: 10.1016/0025-3227(83)90018-X
- Martin D, Bergametti G, Strauss B (1990). On the use of the synoptic vertical velocity in trajectory model: validation by geochemical tracers. *Atmospheric Environment* 24A: 2059-2069. doi: 10.1016/0960-1686(90)90240-N
- McLaren P (1981). An interpretation of trends in grain size measures. *Journal of Sedimentary Research* 51 (2): 611-624. doi: 10.1306/212F7CF2-2B24-11D7-8648000102C1865D
- Moulin C, Lambert CE, Dayan U, Masson V, Ramonet M et al. (1998). Satellite climatology of African dust transport in the Mediterranean atmosphere. *Journal of Geophysical Research* 103 (D11): 13137-13144. doi: 10.1029/98JD00171
- Nickovic S, Jovic D, Kakaliagou O, Kallos G (1997). Production and long-range transport of desert dust in the Mediterranean region: Eta model simulations, 22<sup>nd</sup> NATO / CCMS International Technical Meeting on Air Pollution Modeling and Its Applications, 2-6 June 1997, Clermont-Ferrand, France.
- Okyar M, Ergin M, Evans G (2005). Seismic stratigraphy of Late Quaternary sediments of western Mersin Bay shelf, (NE Mediterranean Sea). *Marine Geology* 220 (1-4): 113-130. doi: 10.1016/j.margeo.2005.06.024
- Özalp I (2009). Limonlu (Lamas) Çayı Havzası'nın Fiziki Coğrafyası. MSc, Atatürk Üniversitesi Sosyal Bilimler Enstitüsü Coğrafya Anabilimdalı (Turkey), p. 167 (in Turkish).
- Palinkas CM, Nittrouer CA (2007). Modern sediment accumulation on the Po shelf, Adriatic Sea, *Continental Shelf Research* 27 (3-4): 489-505. doi: 10.1016/j.csr.2006.11.006
- Pinardi N, Masetti E (2000). Variability of the large scale general circulation of the Mediterranean Sea from observations and modeling: a review *Palaeogeography, Palaeoclimatology, Palaeoecology* 158 (3-4): 153-173. doi: 10.1016/S0031-0182(00)00048-1
- Prospero JM, Nees RT, Mitsuo U (1987). Deposition rate of particulate and dissolved aluminum derived from Saharan dust in precipitation at Miami, FL. *Journal of Geophysical Research* 92: 14723-14731. doi: 10.1029/JD092iD12p14723
- Pye K (1987). *Aeolian Dust and Dust Deposits*. Academic Press, London, 29-62. ISBN 0-12-568690-0
- Pye K (1995). The nature, origin and accumulation of loess. *Quaternary Science Reviews* 14: 653-667. doi: 10.1016 / 0277-3791 (95) 00047-X
- Reiff J, Forbes GS, Spieksma FThM, Reynders JJ (1986). African dust reaching northwestern Europe: a case study to verify trajectory calculations. *Journal of Climate and Applied Meteorology* 25 (11): 1543-1567. doi: 10.1175/1520-0450(1986)025<1543:ADR NEA>2.0.CO;2
- Salihoğlu İ, Yılmaz A, Baştürk Ö, Saydam AC (1987). Kuzey Levant Denizi'nin Oşinografisi. Kimyasal Oşinografi (Volume 2: Technical Report). TÜBİTAK National Marine Surveying and Monitoring Program, Mediterranean sub-project (R83/87-06). METU Institute of Marine Sciences Erdemli-İçel. 125p. (in Turkish).
- Sarnthein M, Tetzlaaf G, Koopman B, Wolter K, Pflaumann U (1981). Glacial and interglacial wind regimes over the eastern subtropical Atlantic and northwest Africa. *Nature* 293: 193-196.

- Shaw HF (1978). The clay mineralogy of the recent surface sediments from the Cilicia Basin, northeastern Mediterranean. *Marine Geology* Volume 26 (3-4): M51-M58. doi: 10.1016/0025-3227(78)90057-9
- Sun D, Bloemendal J, Rea DK, Vandenberghe J, Jiang F et al. (2002). Grain size distribution function of polymodal sediments in hydraulic and aeolian environments, and numerical partitioning of the sedimentary components *Sedimentary Geology* 152 (3-4): 263-277. doi: 10.1016/S0037-0738(02)00082-9
- Swap R, Garstang M, Greco S, Talbot R, Kalberg P (1992). Saharan dust in the Amazon Basin. *Tellus* 44B: 133-149. doi: 10.1029/JC084iC11p06941
- The POEM Group (1992). General circulation of the eastern Mediterranean. *Earth-Science Reviews* 32: 285-308.
- Torres-Padrón ME, Gelado-Caballero MD, Collado-Sanchez C, Siruela-Matos VE, Cardona-Castellano PJ et al. (2002). Variability of dust inputs to the CANIGO zone. *Deep-Sea Res. II*, 49: 3455-3464. doi: 10.1016/S0967-0645(02)00091-7
- Tsoar H, Pye K (1987). Dust transport and the question of desert loess formation. *Sedimentology* 34: 139-153. doi: 10.1111/j.1365-3091.1987.tb00566.x